Cooperative Couplings between Octahedral Rotations and Ferroelectricity in Perovskites and Related Materials

Teng Gu,[1,2] Timothy Scarbrough,[3] Yurong Yang,[3] Jorge Íñiguez,[4] L. Bellaiche,[3,*] and H. J. Xiang[1,2,3,†]
[1]*Key Laboratory of Computational Physical Sciences (Ministry of Education), State Key Laboratory of Surface Physics, and Department of Physics, Fudan University, Shanghai 200433, People's Republic of China*
[2]*Collaborative Innovation Center of Advanced Microstructures, Nanjing 210093, People's Republic of China*
[3]*Physics Department and Institute for Nanoscience and Engineering, University of Arkansas, Fayetteville, Arkansas 72701, USA*
[4]*Materials Research and Technology Department, Luxembourg Institute of Science and Technology (LIST), 41 Rue du Brill, L-4422 Belvaux, Luxembourg*

(Received 22 September 2017; revised manuscript received 18 January 2018; published 10 May 2018)

The structure of ABO_3 perovskites is dominated by two types of unstable modes, namely, the oxygen octahedral rotation (AFD) and ferroelectric (FE) mode. It is generally believed that such AFD and FE modes tend to compete and suppress each other. Here we use first-principles methods to show that a dual nature of the FE-AFD coupling, which turns from competitive to cooperative as the AFD mode strengthens, occurs in numerous perovskite oxides. We provide a unified model of such a dual interaction by introducing novel high-order coupling terms and explain the atomistic origin of the resulting new form of ferroelectricity in terms of universal steric mechanisms. We also predict that such a novel form of ferroelectricity leads to atypical behaviors, such as an enhancement of all the three Cartesian components of the electric polarization under hydrostatic pressure and compressive epitaxial strain.

DOI: 10.1103/PhysRevLett.120.197602

Perovskite-based ferroelectrics (e.g., $BaTiO_3$, $PbTiO_3$, $BiFeO_3$) are the best known and studied ferroelectrics, because they are not only important for applications, but also ideal for understanding the origin of ferroelectricity. In fact, it was demonstrated [1] that the hybridization between the low-lying empty states of the cation (e.g., Ti^{4+}, Pb^{4+}, and Bi^{3+}) and the O $2p$ states (i.e., second-order Jahn-Teller effect [2]) are key factors for the occurrence of ferroelectricity in proper ABO_3 perovskite oxides. It is now therefore widely believed that this feature is essential for proper ferroelectricity to happen in perovskites.

This common belief is, in fact, challenged by the recent experimental discoveries that many ABO_3 with unusually small A ions are polar and/or ferroelectric. For instance, Inaguma *et al.* synthesized [3] $ZnSnO_3$ with a polar $R3c$ $LiNbO_3$-type (LN-type) structure, while Sn^{4+} has no low-lying empty d states and Zn^{2+} does not possess any lone pair. Subsequently, $ZnSnO_3$ thin films [4] were further shown to exhibit a high and switchable FE polarization of $\sim 47\ \mu C/cm^2$. Moreover, the calculated Born effective charges [5] for $ZnSnO_3$ are close to the corresponding nominal charges, confirming that the conventional covalent interaction mechanism is not responsible for ferroelectricity. Strikingly, other LN-type materials with small A ions, such as $ZnPbO_3$ [6,7], $ScFeO_3$ [8,9], $InFeO_3$ [10], $PbNiO_3$ [11] were synthesized. Some of them (e.g., Mn_2FeTaO_6, Zn_2FeOsO_6) [12–14] even simultaneously adopt ordered magnetism, which therefore renders them multiferroic. In these materials, A-site driven FE distortions [Fig. 1(a)] coexist with large antiferrodistortive (AFD) modes [rotations or tilts of the O_6 octahedra, Fig. 1(b)] [15]. However, those two structural distortions are known to typically compete in perovskites [16–19]. Since these ferroelectrics

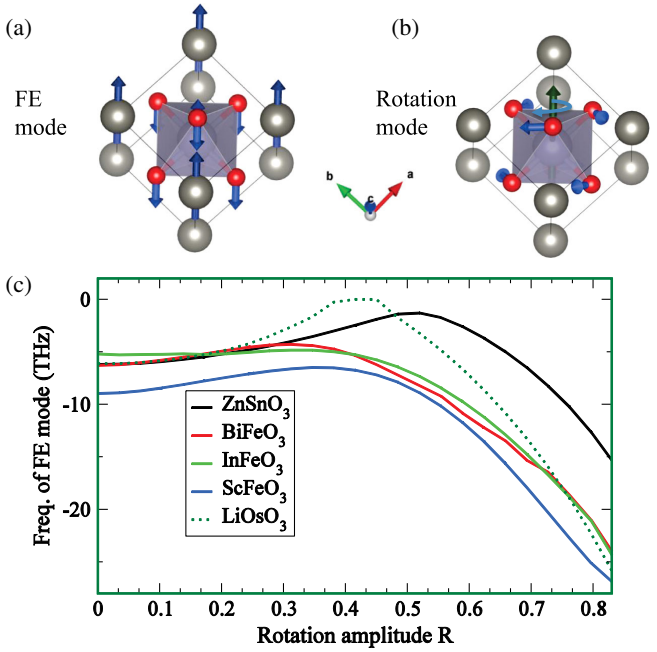

FIG. 1. Schematization of the (a) FE and (b) rotation modes, respectively, and (c) dependence of the frequency of the (unstable) FE mode on the rotation mode in the $R\bar{3}c$ phase of ABO_3.

are promising for the generation of Pb-free ferroelectric thin films and the realization of room-temperature multiferroics, it is highly desirable to understand the mechanism of their ferroelectricity, and why or how the strong FE and large AFD modes can coexist.

In this Letter, we perform density functional theory (DFT) simulations [see Sec. I of the Supplemental Material [20]] to reveal that the FE-AFD couplings follow a universal behavior in many perovskites and related materials, changing from competitive to cooperative as the O_6 tilts increase. In particular, these couplings are found to be cooperative in the regime that is relevant to LN-type compounds like $ZnSnO_3$, and explain the ferroelectric distortion in this and related materials (e.g., the "ferroelectric" metal $LiOsO_3$ [44]). We further show that the cooperative FE-AFD coupling originates from a general steric effect.

Figure 1(c) summarizes our most important result, revealing the dual nature of the FE-AFD couplings for diverse ABO_3 perovskite compounds such as $ZnSnO_3$, $BiFeO_3$, $InFeO_3$, $ScFeO_3$, and $LiOsO_3$. The rhombohedral (noncentrosymmetric) $R3c$ ground states of these compounds can be formed by superimposing two different distortions onto the ideal cubic perovskite structure, as shown in Figs. 1(a) and 1(b): (i) the FE mode that consists of the collective motions of A and B ions along the pseudocubic [111] direction; and (ii) antiphase oxygen octahedral rotations about the pseudocubic [111] direction ($a^-a^-a^-$ pattern in Glazer's notation [45]). To produce Fig. 1(c), we computed the phonon spectrum (e.g., see Fig. S1 of the Supplemental Material [20]) in the $R\bar{3}c$ phases which are obtained by superimposing the $a^-a^-a^-$ tilt (with different amplitude defined with a reduced dimensionless unit [46]) to the ideal cubic perovskite structure [47]. We always observe the same pattern: For relatively small tilts, the frequency of the FE mode along the [111] pseudocubic direction typically grows and approaches zero, implying that the polar instability gets weaker, as consistent with the fact that octahedral tilts have been reported to suppress ferroelectricity in many perovskites (see, e.g., Refs. [15,16,41,48,49]). However, the tendency reverts for relatively large tilts: as the tilting amplitude grows, we obtain more negative frequencies and, correspondingly, stronger FE instabilities. We also examined $LaAlO_3$ and the effect of a ferroelectrically active B ion (i.e., Ti^{4+}) (see Sec. III. 1 of Supplemental Material [20]) to find that the FE-AFD coupling is also cooperative there when the tilt is large. Hence, we find that the FE-AFD competition turns into a strong cooperation for large-enough tilt amplitudes for all investigated compounds (i.e., those examined in Fig. 1(c) and Fig. S8 [20]) with tolerance factors ranging from 0.78 to 1.00 (Table S2 of Supplemental Material [20]).

Having established our basic result, we now focus on $ZnSnO_3$, which is a representative material of LN-type compounds. We note that, while we fully realize that the LN-type and perovskite structures are qualitatively different, here we adopt the approach that LN-type compounds can be thought of as perovskites with very small tolerance factors and large AFD distortions. This will be useful for a unified discussion of the relevant couplings, and to emphasize their observed generality.

Within a reduced dimensionless unit [46], the amplitudes of the FE mode and oxygen octahedral rotation (R) in the $R3c$ ground state of $ZnSnO_3$ are numerically found to be 0.21 and 0.49, respectively. Correspondingly, we obtain the electric polarization to be 55 $\mu C/cm^2$, in agreement with previous experimental [4] (47 $\mu C/cm^2$) and theoretical [5] (57 $\mu C/cm^2$) results, and the rotational angle θ of the oxygen octahedra is as large as ~19° (note that $\tan(\theta) = (\sqrt{2}/2)R$).

To further investigate the dual FE-AFD coupling, we calculate the FE amplitude resulting in the lowest energy for a given rotation amplitude for $R3c$ $ZnSnO_3$. The dependencies of such FE amplitude and corresponding total energy on the rotation amplitude are both shown in Fig. 2(a) (similar results are found for other systems, see Sec. III. 3 of Supplemental Material [20]). Three different structural relaxation strategies are adopted, in order to determine the influence of the lattice vectors on the FE amplitude and total energy: "fix cell," "fix cell shape," and "relax cell." In each of these three cases, the FE mode amplitude is optimized during the structural relaxation while the octahedral rotation amplitude is kept fixed at a given value. These three relaxation schemes differ in the way the cell is relaxed: in the fix cell scheme, the lattice vectors are fixed to that of the paraelectric cubic $Pm\bar{3}m$ structure as obtained from a symmetry-constrained relaxation of $ZnSnO_3$; in the fix cell shape case, the cell is still chosen to be cubic (thus implying that no rhombohedral strain can exist) but its volume can relax; in the relax cell scenario, the lattice vectors are fully optimized. Several interesting trends can be observed from Fig. 2(a): (i) the total energy has a minimum at about $R = 0.5$ for all these three different structural relaxation schemes, which is close to the equilibrium octahedral rotation amplitude in the fully relaxed $R3c$ ground state of $ZnSnO_3$; (ii) the amplitude of the FE mode first decreases and then increases with R, which is in line with the dependence of the phonon frequency on the rotational amplitude depicted in Fig. 1(c). Such nonmonotonic behavior occurs for all three considered elastic constraints, therefore indicating that strain relaxations do not play any qualitative role in the observed dual nature of the FE-AFD coupling, in sharp contrast with the interesting finding for tetragonal $SrTiO_3$ by Aschauer and Spaldin [29]; (iii) the main difference between the different relaxation schemes is that the minimum of the FE mode locates at different rotation amplitudes. In particular, if more strain degrees of freedom are allowed to relax (e.g., if one goes from fix cell to relax cell), the rotation amplitude associated with the minimal value of the FE amplitude becomes smaller. It is also interesting to realize

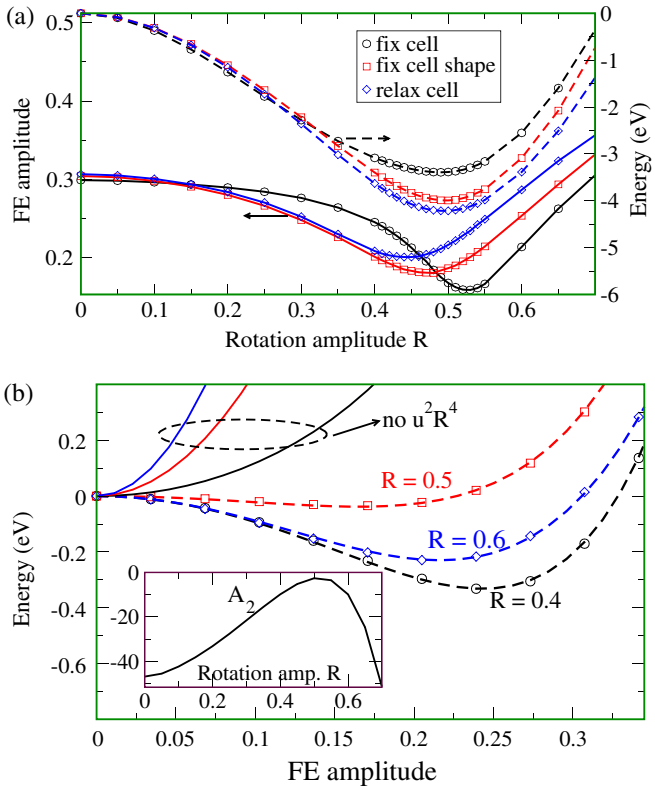

FIG. 2. Couplings between the rotation and FE modes in $R3c$ $ZnSnO_3$. (a) FE amplitude and total energy versus the amplitude of the rotation mode. Three different structural relaxation strategies are chosen (i.e., fix cell, fix cell shape, and relax cell), as explained in the text. (b) Total energy (in eV/10 atoms) as a function of the FE amplitude when the rotation mode is fixed and when choosing the lattice vectors of the cubic relaxed $Pm\bar{3}m$ state of $ZnSnO_3$. Three different rotation amplitudes ($R = 0.4$, 0.5, 0.6) are chosen. Symbols and dashed line represent DFT results and their fit by Eq. (1), respectively. The solid lines are the model results excluding the u^2R^4 term. The inset in panel (b) shows the resulting fitted A_2 parameter (in eV/10 atoms) as a function of the rotational amplitude.

that in the region corresponding to the lowest energies (i.e., for AFD amplitudes around 0.5), the strength of the FE mode increases with R in the relax cell situation while it adopts an opposite behavior in the fix cell scenario. Note that in some systems (e.g., $ScFeO_3$ and $InFeO_3$, see Sec. III. 3 of the Supplemental Material [20]) the tilt magnitude can be large enough to make the overall FE-AFD coupling cooperative even in the fix cell scenario.

In order to better understand the dual nature of the FE-AFD coupling in $R3c$ $ZnSnO_3$, we now introduce a Landau-like potential. More precisely, group theory allows us to derive the following energy expression (up to sixth and fourth orders in FE and AFD mode amplitudes, respectively) for the distorted $R3c$ perovskite structure with respect to the cubic paraelectric state:

$$E(u,R) = A_2(R)u^2 + A_4(R)u^4 + A_6(R)u^6 + E(R), \qquad (1)$$

where u and R represent the amplitudes of the FE and AFD modes, respectively. $E(R)$ characterizes the pure rotational part of energy. $A_2(R) = A_{u^2} + A_{u^2R^2}R^2 + A_{u^2R^4}R^4$, $A_4(R) = A_{u^4} + A_{u^4R^2}R^2 + A_{u^4R^4}R^4$ and $A_6(R) = A_{u^6} + A_{u^6R^2}R^2$, with $A_{u^2R^2}$, $A_{u^2R^4}$, $A_{u^4R^2}$, $A_{u^4R^4}$, and $A_{u^6R^2}$ being coefficients quantifying different FE-AFD couplings. Note that the strain degree of freedom is not explicitly included in this Landau potential, for simplicity and because we showed above that strain does not qualitatively change the dual nature of the FE-AFD coupling. We find that this Landau potential can describe well the FE-AFD interactions. To demonstrate that, we first fix the lattice vectors to be those of the fully relaxed cubic paraelectric $Pm\bar{3}m$ state and report in Fig. 2(b) the total energy of the $R3c$ phase as a function of the FE mode amplitude for three different fixed R values: (i) $R = 0.4$, which falls into the region for which the rotational mode typically suppresses the FE mode [see Fig. 2(a)]; (ii) $R = 0.5$, near which the FE mode has a minimum for the fix cell case of Fig. 2(a); and (iii) $R = 0.6$, for which the AFD mode has the tendency to enhance the FE mode [see Fig. 2(a)]. For each of these three considered R values, the fitted curve (dashed line) of Fig. 2(b) corresponds to the proposed Landau potential and matches very well with the calculated DFT results (shown by means of symbols), therefore supporting the suitability of the model. It can be seen in the inset of Fig. 2(b) that the resulting A_2 parameter (as extracted from the fit of DFT calculations with many different fixed R amplitudes and frozen lattice vectors corresponding to the relaxed cubic paraelectric state) first increases but then decreases with R, while always remaining negative. This naturally implies that $A_{u^2R^2} > 0$ and $A_{u^2R^4} < 0$. The existence of the two couplings $A_{u^2R^2}$ and $A_{u^2R^4}$ having opposite signs evidences the dual nature of the FE-AFD coupling in $ZnSnO_3$: positive $A_{u^2R^2}$ is responsible for the competition between these two modes for smaller R, while negative $A_{u^2R^4}$ testifies of the collaborative nature of the FE and AFD modes for larger R. Note that, if the u^2R^4 term is excluded from the Landau model, the FE mode would be greatly suppressed by the tilt: in fact, we numerically found that there would be no FE instability for $R = 0.4$, 0.5, and 0.6 in that case [see solid lines of Fig. 2(b)], which demonstrates the crucial role that this previously overlooked u^2R^4 coupling plays on ferroelectricity in compounds like $ZnSnO_3$.

To shed further light on this dual nature, we investigate its microscopic mechanism. We find that the dual nature of the FE-AFD coupling has a simple steric origin. In fact, the interaction between the Zn^{2+} and O^{2-} ions includes two contributions, namely, an attractive one (electrostatic or covalent bonding) and a repulsive one (Pauli repulsion). When the rotation amplitude is small (i.e., R smaller than 0.5), the attractive part of potential between Zn and O dominates and the three nearest-neighboring (NN) oxygen ions attract the Zn ion and tend to keep it in plane. In contrast, when the rotation amplitude is large enough (e.g.,

$R = 0.69$), the shortest NN Zn-O distance is smaller than the optimal Zn-O bond length, which results in a repulsive force. The three NN oxygen ions consequently push the central Zn ion out of plane, thus lowering the repulsive contribution to the energy and inducing an electric polarization along the pseudocubic [111] direction (see Sec. II of the Supplemental Material for a detailed discussion [20]). This is different from the small (even zero) AFD rotation case where the proper ferroelectricity in $ZnSnO_3$ is due to the fact that the Zn ion is undercoordinated (The Zn ion tends to move closer to oxygen ions and form bonds with them).

Note that Benedek and Fennie [15] also noticed the local environment of the Zn ion in the $R\bar{3}c$ structure of $ZnSnO_3$. They proposed that the driving force for the FE instability in $R\bar{3}c$ structure can be understood from bond valence arguments. However, they did not appreciate the collaborative effect between AFD and FE modes to explain ferroelectricity in $ZnSnO_3$. In fact, they used a Landau-like model only up to fourth order, which excludes the presence of the u^2R^4 term required to reproduce the dual-coupling behavior that we observe. We further show that the FE-AFD dual coupling also exists for tilt patterns other than the $a^-a^-a^-$ tilt (Sec. II. 2 of Supplemental Material [20]). A theoretical work [29] on $SrTiO_3$ suggests that FE and AFD modes may actually cooperate because of an effect mediated by strain if one were able to access a suitable regime. However, our proposed steric effect (not necessarily involving strain) responsible for the FE-AFD cooperation is more general than and different from the special strain mechanism for $SrTiO_3$ (see Sec. III. 2 of the Supplemental Material [20]).

The novel FE-AFD cooperative coupling revealed in this work also leads to atypical effects. It is well known that hydrostatic pressure typically weakens or even suppresses electrical polarization in most perovskites [50,51], since the short-range repulsions (favoring a paraelectric state) increase more rapidly than long-range interactions (preferring a FE state) as pressure increases. On the other hand, improper ferroelectricity in hexagonal $ReMnO_3$ and $ReFeO_3$ (Re stands for a rare-earth element) was found to be stronger under compression [52,53], as a result of the concomitant enhancement of the primary K_3 AFD tilting mode. In view of such an interesting behavior, one may wonder how pressure will affect ferroelectricity in LN-type compounds. Indeed, while being proper in nature, we find that ferroelectricity in materials like $ZnSnO_3$ is linked to the amplitude of the nonpolar AFD distortion, and the FE response to any external perturbation should thus be conditioned by the response of the tilting modes. To address such an issue, the FE polarization and AFD rotation amplitudes in the $R3c$ state of $ZnSnO_3$ are shown in Fig. 3 as a function of hydrostatic pressure up to 80 kbar. Three different ways to relax the structures are adopted here: (i) both atomic positions and lattice vectors are fully relaxed, which is denoted as the full relax case in Fig. 3(a); (ii) the lattice vectors are optimized and atomic positions are relaxed, except those related to the AFD rotation, which are fixed to be equal to their zero-pressure values; this situation is termed fix rotation here; and (iii) the cell shape is taken to be cubic, while the atomic positions and the volume of such a cubic cell are allowed to relax in order to minimize the energy; such a case is denoted fix cell shape. In all these three cases, Fig. 3 indicates that the electrical polarization increases with the hydrostatic pressure, which constitutes a novel effect for proper ferroelectrics. When no rhombohedral distortion is allowed (i.e., in the fix cell shape scenario), the magnitude of the FE polarization is smaller than in the other two cases, but the polarization-versus-pressure curve has a similar slope. Note that we also found that the octahedral rotation amplitude increases with pressure in the full relax case; however, such an increase is tiny, which explains why the electric polarization is almost identical in the full relax and fix rotation cases. We show that the fact that $A_{u^2R^4}$ quickly decreases when reducing the lattice constant [mechanism III in Fig. 3(c)] constitutes the main and novel mechanism responsible for the unusual enhancement of polarization under pressure (see Sec. II. 5 of the Supplemental Material [20]).

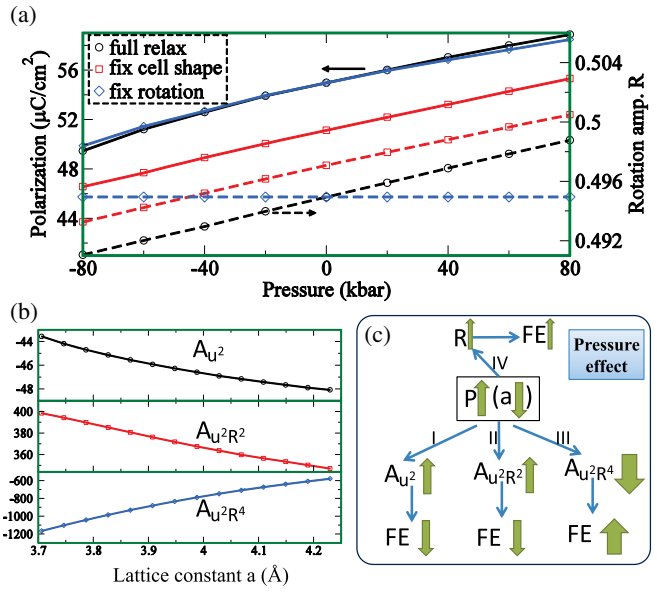

FIG. 3. Pressure behavior of the electrical polarization in $R3c$ $ZnSnO_3$. (a) Amplitudes of the polarization (solid lines) and rotation (dashed lines) as a function of pressure. Three different ways for structural optimization are adopted, namely, fix cell shape, full relax, and fix rotation (see text). (b) Coefficients (A_{u^2}, $A_{u^2R^2}$, and $A_{u^2R^4}$) related to the second order u^2 terms as a function of the cubic lattice constant. (c) Schematization of four different mechanisms for the pressure effect on the FE polarization. In $ZnSnO_3$, $A_{u^2R^4}$ decreases quickly with pressure, which is mainly responsible for the enhancement of FE polarization by pressure.

In addition, we discover that a compressive epitaxial strain enhances not only the out-of-plane polarization, but also the in-plane components of the polarization since the compressive strain enhances the $a^0a^0c^-$ octahedron rotation, which subsequently leads to an enhancement of the in-plane FE polarizations as a result of the cooperative $-u^2R^4$ term (see Sec. II. 6 of the Supplemental Material [20]). The dual FE-AFD coupling may also result in unusual finite-temperature effects. For instance, the $R3c$ phase appears to have a higher T_c than the $P4mm$ phase without tilt even though the $P4mm$ phase has a larger polarization than the $R3c$ phase (see Sec. IV of Supplemental Material [20]).

In summary, we reveal the dual nature of the FE-AFD coupling in many ABO_3 perovskites. We dispute the common knowledge that FE-AFD couplings are always competitive in any regime of practical importance. In fact, we show that, while the large-AFD range is not relevant for some common perovskites (like, e.g., $CaTiO_3$ or $SrTiO_3$), it does apply to all-important recently synthesized $LiNbO_3$-like compounds (like, e.g., $ZnSnO_3$ or $LiOsO_3$) that display a noncentrosymmetric ground state combining AFD and FE distortions.

Work at Fudan is supported by NSFC (11374056), the Special Funds for Major State Basic Research (2015CB921700), Program for Professor of Special Appointment (Eastern Scholar), Qing Nian Ba Jian Program, and Fok Ying Tung Education Foundation. H. X. and T. S. also thank the support of the Department of Energy, Office of Basic Energy Sciences, under Award No. DE-SC0002220. Y. Y. acknowledges the ONR Grants No. N00014-12-1-1034 and No. N00014-17-1-2818. L. B. thanks the Air Force Office of Scientific Research under Grant No. FA9550-16-1-0065. We also acknowledge funding from the Luxembourg National Research Fund through the inter-mobility (Grant No. 15/9890527 GREENOX, J. I. and L. B.) and Pearl (Grant No. P12/4853155 COFERMAT, J. I.) programs. Some computations were also made possible owing to MRI Grant No. 0722625 from NSF, ONR Grant No. N00014-15-1-2881 (DURIP), and a Challenge grant from the Department of Defense.

*laurent@uark.edu
†hxiang@fudan.edu.cn

[1] R. E. Cohen, Nature (London) **358**, 136 (1992).
[2] J. M. Rondinelli, A. S. Eidelson, and N. A. Spaldin, Phys. Rev. B **79**, 205119 (2009).
[3] Y. Inaguma, M. Yoshida, and T. Katsumata, J. Am. Chem. Soc. **130**, 6704 (2008).
[4] J. Y. Son, G. Lee, M.-H. Jo, H. Kim, H. M. Jang, and Y.-H. Shin, J. Am. Chem. Soc. **131**, 8386 (2009).
[5] M. Nakayama, M. Nogami, M. Yoshida, T. Katsumata, and Y. Inaguma, Adv. Mater. **22**, 2579 (2010).
[6] R. Yu, H. Hojo, T. Mizoguchi, and M. Azuma, J. Appl. Phys. **118**, 094103 (2015).
[7] D. Mori, K. Tanaka, H. Saitoh, T. Kikegawa, and Y. Inaguma, Inorg. Chem. **54**, 11405 (2015).
[8] M.-R. Li *et al.*, J. Am. Chem. Soc. **134**, 3737 (2012).
[9] T. Kawamoto *et al.*, J. Am. Chem. Soc. **136**, 15291 (2014).
[10] K. Fujita *et al.*, Chem. Mater. **28**, 6644 (2016).
[11] Y. Inaguma, K. Tanaka, T. Tsuchiya, D. Mori, T. Katsumata, T. Ohba, K.-i. Hiraki, T. Takahashi, and H. Saitoh, J. Am. Chem. Soc. **133**, 16920 (2011).
[12] M.-R. Li, P. W. Stephens, M. Retuerto, T. Sarkar, C. P. Grams, J. Hemberger, M. C. Croft, D. Walker, and M. Greenblatt, J. Am. Chem. Soc. **136**, 8508 (2014).
[13] M.-R. Li *et al.*, Angew. Chem., Int. Ed. **52**, 8406 (2013).
[14] P. S. Wang, W. Ren, L. Bellaiche, and H. J. Xiang, Phys. Rev. Lett. **114**, 147204 (2015).
[15] N. A. Benedek and C. J. Fennie, J. Phys. Chem. C **117**, 13339 (2013).
[16] I. A. Kornev, L. Bellaiche, P. E. Janolin, B. Dkhil, and E. Suard, Phys. Rev. Lett. **97**, 157601 (2006).
[17] W. Zhong and D. Vanderbilt, Phys. Rev. Lett. **74**, 2587 (1995).
[18] N. Sai and D. Vanderbilt, Phys. Rev. B **62**, 13942 (2000).
[19] J. C. Wojdeł, P. Hermet, M. P. Ljungberg, P. Ghosez, and J. Íñiguez, J. Phys. Condens. Matter **25**, 305401 (2013).
[20] See Supplemental Material at http://link.aps.org/supplemental/10.1103/PhysRevLett.120.197602, which includes Refs. [21–43], for computational details, phonon dispersion, self-force constants, effect of compressive strain on the ferroelectric polarization of the (001) $ZnSnO_3$ thin film, dependence of the frequency of the FE modes on the rotation modes in $ATiO_3$ and $LaAlO_3$, finite-temperature properties obtained with an effective Hamiltonian.
[21] P. E. Blöchl, Phys. Rev. B **50**, 17953 (1994).
[22] G. Kresse and J. Furthmüller, Phys. Rev. B **54**, 11169 (1996).
[23] G. Kresse and J. Furthmüller, Comput. Mater. Sci. **6**, 15 (1996).
[24] G. Kresse and D. Joubert, Phys. Rev. B **59**, 1758 (1999).
[25] J. P. Perdew, K. Burke, and M. Ernzerhof, Phys. Rev. Lett. **77**, 3865 (1996).
[26] R. D. King-Smith and D. Vanderbilt, Phys. Rev. B **47**, 1651 (1993).
[27] D. Vanderbilt and R. D. King-Smith, Phys. Rev. B **48**, 4442 (1993).
[28] R. Resta, Rev. Mod. Phys. **66**, 899 (1994).
[29] U. Aschauer and N. A. Spaldin, J. Phys. Condens. Matter **26**, 122203 (2014).
[30] J. P. Perdew, A. Ruzsinszky, G. I. Csonka, O. A. Vydrov, G. E. Scuseria, L. A. Constantin, X. Zhou, and K. Burke, Phys. Rev. Lett. **100**, 136406 (2008).
[31] K. Parlinski, Z. Q. Li, and Y. Kawazoe, Phys. Rev. Lett. **78**, 4063 (1997).
[32] A. Togo, F. Oba, and I. Tanaka, Phys. Rev. B **78**, 134106 (2008).
[33] R. D. Shannon, Acta. Cryst. **A32**, 751 (1976).
[34] P. Hohenberg and W. Kohn, Phys. Rev. **136**, B864 (1964).
[35] W. Kohn and L. J. Sham, Phys. Rev. **140**, A1133 (1965).
[36] B. Dupé, S. Prosandeev, G. Geneste, B. Dkhil, and L. Bellaiche, Phys. Rev. Lett. **106**, 237601 (2011).
[37] A. J. Hatt, N. A. Spaldin, and C. Ederer, Phys. Rev. B **81**, 054109 (2010).

[38] C. Ederer and N. A. Spaldin, Phys. Rev. Lett. **95**, 257601 (2005).
[39] R. A. Cowley, Phys. Rev. **134**, A981 (1964).
[40] L. Bellaiche and J. Íñiguez, Phys. Rev. B **88**, 014104 (2013).
[41] W. Zhong, D. Vanderbilt, and K. M. Rabe, Phys. Rev. B **52**, 6301 (1995).
[42] L. Bellaiche, A. García, and D. Vanderbilt, Phys. Rev. Lett. **84**, 5427 (2000).
[43] K. Hukushima and K. Nemoto, J. Phys. Soc. Jpn. **65**, 1604 (1996).
[44] Y. Shi *et al.*, Nat. Mater. **12**, 1024 (2013).
[45] A. M. Glazer, Acta Crystallogr. Sect. B **28**, 3384 (1972).
[46] The magnitude of the mode is defined to be 1 if the sum of the square of the displacements equal to the square of the cubic lattice constant.
[47] We first optimize the lattice constants of the ideal cubic ($Pm\bar{3}m$) perovskite structures for each of the considered materials.
[48] D. Vanderbilt and W. Zhong, Ferroelectrics **206**, 181 (1998).
[49] S. Amisi, E. Bousquet, K. Katcho, and P. Ghosez, Phys. Rev. B **85**, 064112 (2012).
[50] E. Bousquet and P. Ghosez, Phys. Rev. B **74**, 180101 (2006).
[51] G. A. Samara, T. Sakudo, and K. Yoshimitsu, Phys. Rev. Lett. **35**, 1767 (1975).
[52] C. Xu, Y. Yang, S. Wang, W. Duan, B. Gu, and L. Bellaiche, Phys. Rev. B **89**, 205122 (2014).
[53] H. Tan, C. Xu, M. Li, S. Wang, B.-L. Gu, and W. Duan, J. Phys. Condens. Matter **28**, 126002 (2016).